

Carbon dynamics and CO₂ air-sea exchanges in the eutrophied coastal waters of the Southern Bight of the North Sea: a modelling study

N. Gypens¹, C. Lancelot¹, and A. V. Borges²

¹Université Libre de Bruxelles, Ecologie des Systèmes Aquatiques, CP-221, Bd du Triomphe, B-1050, Belgium

²Université de Liège, MARE, Unité d'Océanographie Chimique, Institut de Physique (B5), B-4000 Sart Tilman, Belgium

Received: 16 August 2004 – Published in Biogeosciences Discussions: 7 September 2004

Revised: 6 December 2004 – Accepted: 20 December 2004 – Published: 23 December 2004

Abstract. A description of the carbonate system has been incorporated in the MIRO biogeochemical model to investigate the contribution of diatom and *Phaeocystis* blooms to the seasonal dynamics of air-sea CO₂ exchanges in the Eastern Channel and Southern Bight of the North Sea, with focus on the eutrophied Belgian coastal waters. For this application, the model was implemented in a simplified three-box representation of the hydrodynamics with the open ocean boundary box 'Western English Channel' (WCH) and the 'French Coastal Zone' (FCZ) and 'Belgian Coastal Zone' (BCZ) boxes receiving carbon and nutrients from the rivers Seine and Scheldt, respectively. Results were obtained by running the model for the 1996–1999 period. The simulated partial pressures of CO₂ (pCO₂) were successfully compared with data recorded over the same period in the central BCZ at station 330 (51°26.05' N; 002°48.50' E). Budget calculations based on model simulations of carbon flow rates indicated for BCZ a low annual sink of atmospheric CO₂ ($-0.17 \text{ mol C m}^{-2} \text{ y}^{-1}$). On the opposite, surface water pCO₂ in WCH was estimated to be at annual equilibrium with respect to atmospheric CO₂. The relative contribution of biological, chemical and physical processes to the modelled seasonal variability of pCO₂ in BCZ was further explored by running model scenarios with separate closures of biological activities and/or river inputs of carbon. The suppression of biological processes reversed direction of the CO₂ flux in BCZ that became, on an annual scale, a significant source for atmospheric CO₂ ($+0.53 \text{ mol C m}^{-2} \text{ y}^{-1}$). Overall biological activity had a stronger influence on the modelled seasonal cycle of pCO₂ than temperature. Especially *Phaeocystis* colonies which growth in spring were associated with an important sink of atmospheric CO₂ that counteracted the temperature-driven increase of pCO₂ at this period of the year. However, river inputs of organic and inorganic carbon

were shown to increase the surface water pCO₂ and hence the emission of CO₂ to the atmosphere. Same calculations conducted in WCH, showed that temperature was the main factor controlling the seasonal pCO₂ cycle in these open ocean waters. The effect of interannual variations of fresh water discharge (and related nutrient and carbon inputs), temperature and wind speed was further explored by running scenarios with forcing typical of two contrasted years (1996 and 1999). Based on these simulations, the model predicts significant variations in the intensity and direction of the annual air-sea CO₂ flux.

1 Introduction

Coastal waters are heavily impacted by nutrients and carbon inputs from rivers and estuaries that stimulate production and remineralization of organic matter. They also intensively exchange nutrients, and inorganic and organic carbon with the open ocean across marginal boundaries (e.g. Thomas et al., 2004a). Consequently, these areas play a key role in the global carbon cycle by linking the terrestrial, oceanic and atmospheric reservoirs (Gattuso et al., 1998; Mackenzie et al., 2004). There is nowadays a great uncertainty on the overall role of coastal ecosystems to act as a sink or a source for atmospheric CO₂ due to the large variability of recorded air-sea CO₂ exchanges across latitudinal and ecosystem gradients. Existing data of CO₂ air-sea fluxes suggest that temperate marginal seas act as sinks for atmospheric CO₂ (Tsunogai et al., 1999; Frankignoulle and Borges, 2001a; Borges and Frankignoulle, 2002a; DeGranpre et al., 2002; Thomas et al., 2004a, b). On the contrary sub-tropical marginal seas (Cai et al., 2003) and near-shore aquatic ecosystems influenced by terrestrial inputs such as inner and outer estuaries (Frankignoulle et al., 1998; Cai et al., 2000; Raymond et al., 2000; Borges and Frankignoulle 2002b; Bouillon et al., 2003), mangroves (Borges et al., 2003) and non-estuarine

Correspondence to: N. Gypens
(ngypens@ulb.ac.be)

salt marshes (Wang and Cai, 2004) act as sources of CO₂ to the atmosphere. However, the paucity of field data prevents the comprehensive biogeochemical description of the very diverse coastal ecosystems that is needed for the integration of CO₂ fluxes on a global scale. Furthermore, little is known on the seasonal and interannual variability of CO₂ dynamics and fluxes in coastal ecosystems, although it has been shown to be highly significant in open oceanic waters in relation to large scale climatic forcings acting at various time-scales (e.g. Takahashi et al., 2003). In the absence of long term time-series, these aspects of CO₂ cycling in coastal ecosystems can only be approached with modelling tools (e.g. Ianson and Allen, 2002). Up to now, little mechanistic modelling effort has been devoted to the description of the dynamics of dissolved inorganic carbon (DIC) in coastal environments (Walsh et al., 1994, 1996; Mackenzie et al., 2004).

The North Sea is amongst the best-studied coastal areas in the World, with respect to its physical, chemical and biological characteristics. However, the spatio-temporal monitoring of DIC has been limited to near-shore waters such as the German Bight, the Wadden Sea or the Belgian coastal zone (Hoppema, 1991; Borges and Frankignoulle, 1999, 2002b; Brasse et al., 2002). Recently the seasonality of pCO₂ has been investigated in the whole North Sea (Thomas et al., 2004b). On this basis a detailed carbon budget that identifies the major players in the large scale air-sea CO₂ fluxes has been established (Thomas et al., 2004b). Results point the Southern Bight as distinct from the Northern North Sea in terms of organic and inorganic carbon cycling. This is related to both their different hydrographic features (permanently well-mixed shallow versus seasonally-stratified water column, in the South and North, respectively) and the influence of rivers inputs that are concentrated in the Southern Bight.

The Belgian coastal zone (BCZ) located in the Southern Bight of the North Sea is a highly dynamic system with water masses resulting from the variable mixing between the inflowing southwest Atlantic waters through the Strait of Dover and the Scheldt freshwater and nutrient inputs. The inflowing Atlantic waters are themselves enriched with nutrient inputs from the river Seine (Lancelot et al., 1987). The river inputs characterized by a large excess of nitrate over phosphate and silicate are shaping the structure and the functioning of the ecosystem characterized by the dominance of undesirable recurrent blooms of non-siliceous phytoplankton like *Phaeocystis* colonies (Lancelot, 1995).

In this paper, we test a complex biogeochemical model (MIRO-CO₂) to investigate the present-day impact of land-based nutrients and carbon inputs from the Seine and Scheldt rivers on the functioning of the *Phaeocystis*-dominated ecosystem of the Southern Bight of the North Sea and the related air-sea CO₂ exchanges. The model is run over the 1996–1999 period when existing field data of CO₂ partial pressure (pCO₂) allow model validation. We further conduct

model scenarios to evaluate the respective contribution of biological, chemical and physical processes to the seasonal and annual variability of pCO₂. Finally, we investigate the impact of the hydro-climatic constraints (river inputs, temperature, wind stress) on the pCO₂ seasonal dynamics by running scenarios with contrasting but realistic meteorological conditions.

2 Material and method

2.1 Model description

The MIRO-CO₂ biogeochemical model results of the coupling of the detailed biogeochemical MIRO model (Lancelot et al., 2004) with the physico-chemical module of Hannon et al. (2001) detailing the seawater carbonate system and air-sea CO₂ exchange. MIRO is a mechanistic model that describes C, N, P and Si cycling through aggregated components of the *Phaeocystis*-dominated ecosystem of the North Sea. It includes thirty-two state variables assembled in four modules expressing the dynamics of phytoplankton, zooplankton, organic matter degradation and nutrients (NO₃, NH₄, PO₄ and SiO), regeneration by bacteria in the water column and the sediment. The phytoplankton module considers three phytoplankton groups (diatoms, free-living autotrophic nanoflagellates and *Phaeocystis* colonies) the growth physiology of which is described according to the AQUAPHY model of Lancelot et al. (1991). The latter model considers 3 intracellular constituents (small metabolites, reserve material, functional and structural metabolites) and distinguishes different processes: photosynthesis, reserve synthesis and catabolism, growth and associated nutrient uptake, respiration and lysis. The zooplankton module details the dynamics of two groups: the microzooplankton feeding on free-living autotrophic nanoflagellates and bacteria and the mesozooplankton grazing on diatoms and microzooplankton. *Phaeocystis* colonies escape grazing, but are submitted to colony disruption which releases in the ambient nanoflagellated cells and organic matter. The degradation of organic matter by planktonic bacteria is described according to the HSB model (Billen and Servais, 1989), considering two classes of biodegradability for both dissolved and particulate organic matter. Benthic organic matter degradation and nutrient recycling are calculated using the algorithms developed by Lancelot and Billen (1985) and Billen et al. (1989).

The physico-chemical module of Hannon et al. (2001) details the carbonate system in seawater and calculates CO₂ exchange between the surface water and the atmosphere. The speciation of the carbonate system (in particular pCO₂) is calculated based on the knowledge of DIC and total alkalinity (TA), using stoichiometric relationships and apparent equilibrium constants, which are function of temperature, pressure and salinity (Weiss, 1974; Millero et al., 1993). DIC and TA are computed taking into account, respectively, the

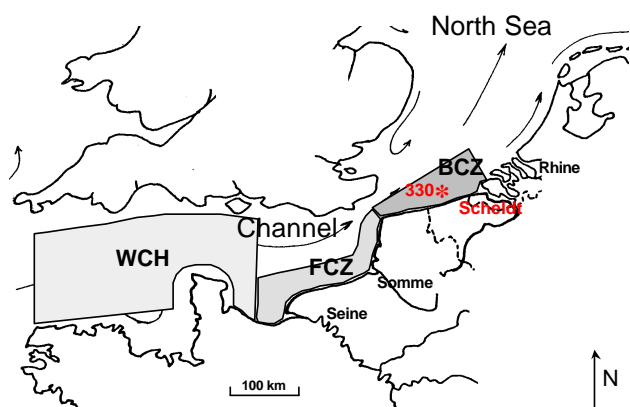


Fig. 1. Map of the studied area showing the MIRO multi-box frame (adapted from Lancelot et al., 2004) and the location of the station 330 (51°26.05' N; 002°48.50' E).

biological uptake or release of carbon and the phytoplankton assimilation of nitrate, all provided by the MIRO model. Air-sea CO₂ fluxes are calculated from the pCO₂ gradient across the air-sea interface and the gas transfer velocity estimated from wind speed and using the parameterisation of Nightingale et al. (2000). The latter was chosen among several existing empirical formulations since it was established from dual tracer experiments in the Southern Bight of the North Sea.

2.2 Model runs

The MIRO-CO₂ model was applied in the coastal domain of the eastern English Channel and Southern Bight of the North Sea, between the Baie de Seine and the northern limit of BCZ (Fig. 1). The model was implemented in a multi-box frame delineated on the basis of the hydrological regime and the river inputs. In order to take into account the cumulated nutrient enrichment of Atlantic waters by the Seine and Scheldt rivers, two successive boxes, assumed to be homogeneous, were chosen from the Baie de Seine to the BCZ (Fig. 1). Each successive box was characterized by its own area, depth, water temperature and average salinity, light conditions and water residence time and was treated as an open system, receiving water from the southern adjacent box and exporting water to the northern box (Lancelot et al., 2004). The boundary conditions were provided by the results of the calculations performed for the conditions existing in the Western Channel area, considered as a quasi-oceanic closed system. Initial conditions of nutrients were extracted from the database of Radach et al. (1995). Initial conditions of DIC (2070 mmol C m⁻³) and total alkalinity (2290 mmol m⁻³) were estimated from existing data in the area for the 1996–1999 period (Borges and Frankignoulle, 2003). The seasonal variation of the state variables was calculated by solving the equations expressing mass conservation, according to the Euler procedure, with a time step of

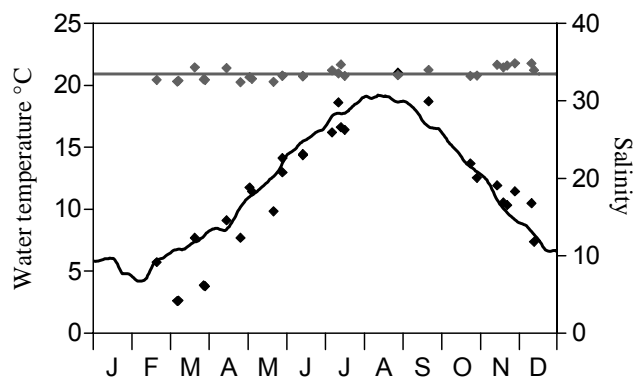


Fig. 2. Modelled (solid line for BCZ) and observed (♦ at station 330) temperature (black) and salinity (grey).

15 min. Conservation equations and parameters are detailed in Lancelot et al. (2004).

Model simulations were run with 1996–1999 climatological forcings for hydro-meteorological conditions and river inputs. These functions were computed from recorded daily global solar radiation (Oostende Station, Institut Royal de Météorologie, Belgium), seawater temperature and monthly nutrient loads for the rivers Seine (Cellule Antipollution de Rouen du Service de la Navigation de la Seine, France) and Scheldt [Institute for Inland Water Management and Waste Water Treatment, The Netherlands) and Department of Environment and Infrastructure (Ministry of Flemish Community, Belgium). Organic carbon loads by the Scheldt were retrieved from the Dutch water base (<http://www.waterbase.nl>). For the river Seine, we used data described in Servais et al. (2003). Land-based fluxes of DIC and TA were estimated based on a compilation of DIC and TA concentrations in the Seine and the Scheldt rivers (Frankignoulle et al., 1996, 1998; Frankignoulle and Borges, 2001b; Abril, personal communication) and river discharges, making use of the “apparent zero end-member” method (Kaul and Froelich, 1984). Atmospheric pCO₂ was extracted from the Mace Head (53°33' N 9°00' W, Southern Ireland) and the National Oceanic and Atmospheric Administration/climate Monitoring and Diagnostics Laboratory/Carbon Cycle Greenhouse Gases Group (NOAA/CMDL/CCGG) air sampling network (available at <http://www.cmdl.noaa.gov/>). Wind speed at 50.0° N 6.0° W was provided by the Pacific Fisheries Environmental Laboratory (PFEL) and is based on Fleet Numerical Meteorology and Oceanography Center (FNMOC) synoptic pressure fields.

2.3 Validation data

Model results were daily-averaged and compared with available data sets in the central BCZ at the station 330 (51°26.05 N; 02°48.50 E) for the 1996–1999 period. Over this period, nutrients, phytoplankton and chlorophyll data

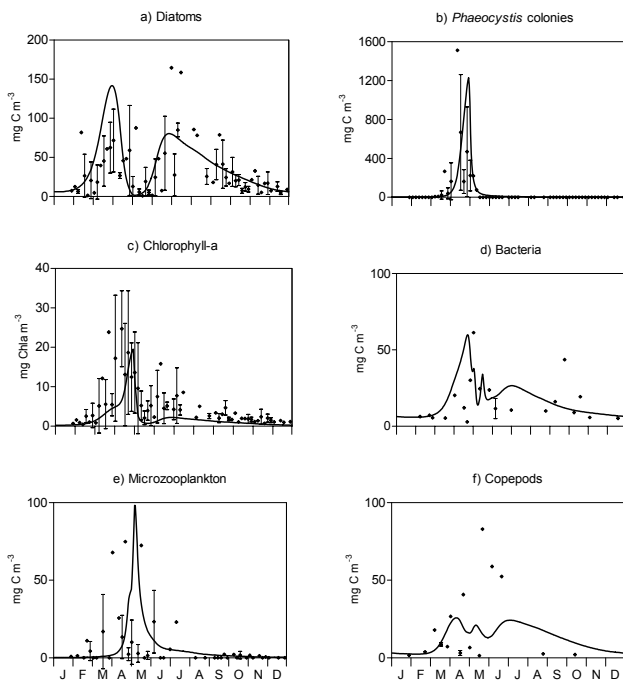


Fig. 3. Model results in BCZ (solid line) and observations 5-day average and standard deviation over 1996–1999 (◆) of (a) diatoms, (b) *Phaeocystis* colonies, (c) Chlorophyll-*a*, (d) bacteria, (e) microzooplankton and (f) copepods at the station 330 for the 1996–1999 period.

were collected at a weekly frequency except during winter when bimonthly (Rousseau, 2000). DIC was calculated from TA and pCO₂ measured between 1996 and 1999 in the BCZ and WCH (Borges and Frankignoulle, 1999, 2002b, 2003). Due to the inherent discrepancy between in situ temperature at the time of pCO₂ measurement and that imposed by the climatological forcing of the model (Fig. 2), field data of pCO₂ were corrected with respect to the modelled temperature. Similarly, DIC and TA data obtained at station 330 were normalized to the mean BCZ salinity of 33.5 imposed by the chosen box-model implementation in order to overcome the effect of salinity discrepancy (Fig. 2). The normalized DIC and TA are written DIC_(33.5) and TA_(33.5).

3 Results and discussion

3.1 Model validation

3.1.1 Biological state variables

Figure 3 compares MIRO-CO₂ predictions of diatom (Fig. 3a) and *Phaeocystis* (Fig. 3b) biomass, total phytoplankton (mg Chl *a* m⁻³, Fig. 3c), bacteria (Fig. 3d), microzooplankton (Fig. 3e) and copepods (Fig. 3f) biomass with field data collected between 1996 and 1999. The model

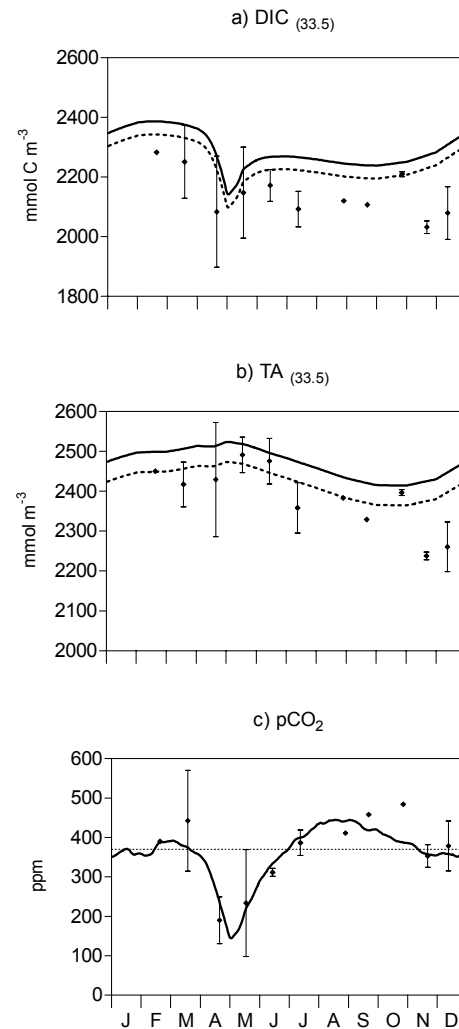


Fig. 4. Model results (solid line) and observations (◆) of (a) dissolved inorganic carbon DIC_(33.5), (b) total alkalinity TA_(33.5) and (c) surface water pCO₂. The dotted line corresponds to the atmospheric equilibrium. Modelled results of sensitivity test were added (dotted line) on (a) DIC_(33.5), (b) TA_(33.5) plots.

describes reasonably well the main trends (timing and magnitude) of the diatom-*Phaeocystis*-diatom succession: spring diatoms (Fig. 3a) initiate the phytoplankton bloom in early March and are followed by *Phaeocystis* colonies (Fig. 3b) which reach concentrations of 20 mg Chl *a* m⁻³ in April (Fig. 3c). Summer diatoms bloom after *Phaeocystis* decline and maintain up to fall. In agreement with observations, MIRO-CO₂ results show non-negligible concentration of diatoms all over the year (Fig. 3a) contrasting with the unique bloom of *Phaeocystis* in spring (Fig. 3b). Phytoplankton decline in spring stimulates the development of diverse heterotrophs such as bacteria (Fig. 3d), microzooplankton (Fig. 3e) and copepods (Fig. 3f). The seasonal succession and magnitude of spring bacteria and microzooplankton biomass are well captured by the model. However, biomass

reached by copepods and bacteria in spring and fall, respectively, are not properly simulated. These weaknesses of the model are discussed in Lancelot et al. (2004) and is mainly attributed to some mismatch between the simulated seasonal succession of copepods and their prey which might be related to some unreliable description of either the mortality process and fate of *Phaeocystis* colonies and derived matter and/or the copepod feeding function. Experimental work in this matter is in progress.

3.1.2 Carbonate chemistry

Figure 4 compares MIRO-CO₂ simulations of DIC_(33.5) (Fig. 4a), TA_(33.5) (Fig. 4b) and surface water pCO₂ (Fig. 4c) with field observations. The seasonal evolution of DIC_(33.5) and TA_(33.5) is reasonably well captured by the model but concentrations obtained overestimate field data, especially in winter and late fall (Fig. 4a, b) when biological activity is low (Fig. 3). The simulated DIC_(33.5) clearly reaches lowest values at the time of *Phaeocystis* bloom maximum (Fig. 3b; Fig. 4a) and increases in mid-May when heterotrophs prevail over autotrophs (Fig. 4a; Fig. 3d, e, f). In agreement the highest TA_(33.5) values (Fig. 4a) are modelled in end April-early May when phytoplankton biomass is elevated (Fig. 3a, b, c) and consumes NO₃. Lowest TA_(33.5) are simulated in late fall (Fig. 4b) when phytoplankton growth has ceased but heterotrophic process and nitrification are still operating. The observed seasonal signal of TA_(33.5) is well represented (Fig. 4b) but the modelled amplitude (110 mmol m⁻³) is weak compared to that suggested by field data (~200 mmol m⁻³, Fig. 4b), mainly because of the failure of the model to capture the observed late fall-winter minima (Fig. 4b). At the annual scale, Atlantic waters bring 96% of TA in BCZ and river loads and biological processes contribute 3.9% and 0.1%, respectively. Sensitivity tests with varying initial TA corresponding to the range of observed values in WCH (Borges and Frankignoulle, 2003) indicate that a reduction of WCH initial conditions of TA by less than 2% improves significantly model simulations of DIC (Fig. 4a) and TA (Fig. 4b) in winter while fall observations remain overestimated by the model (Fig. 4a, b). Elevated modelled TA in fall could result from an overestimation of river inputs during this period. At that time of the year (October to January), river discharge is high and inputs of TA account for 45% of annual river loads. Due to the importance of biological processes on magnitude and seasonal variability of DIC, modification of DIC initial value in the Western Channel has no impact on DIC magnitude in the Belgian coastal zone.

The discrepancies in the BCZ between observed and modelled DIC and TA are due to the structure of the model since initial conditions are not forced in the BCZ but result from the transformations of chemical water properties from the WCH (model initial conditions) due to river inputs and biological activity during transport through the FCZ and BCZ

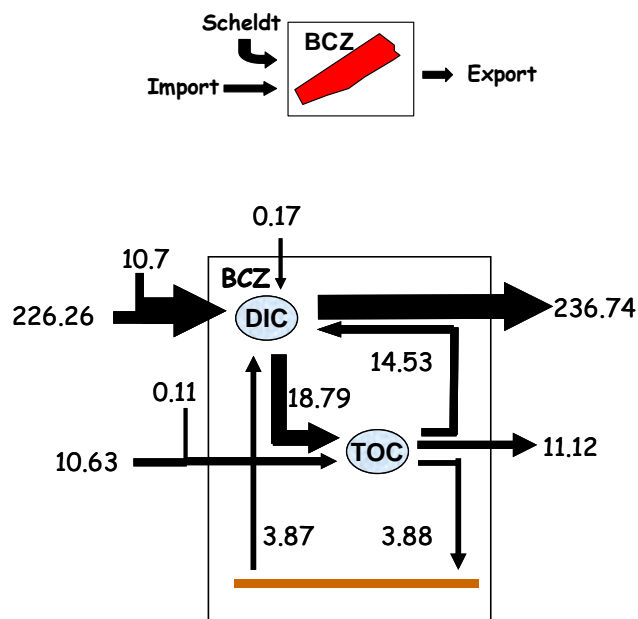


Fig. 5. Annual budget of C flows at the scale of the BCZ (mol C m⁻² y⁻¹).

boxes. Altogether, these discrepancies between observed and modelled DIC and TA have no influence on the magnitude and seasonal evolution of the modelled pCO₂.

The comparison between modelled and measured pCO₂ (Fig. 4c) shows that our model is able to describe the observed seasonal variability, both in time and amplitude. The latter (defined as the difference between the maximum and minimum values) is evaluated at 300 ppm with pCO₂ values ranging between 445 ppm in summer and 145 ppm in spring (Fig. 4c). Model pCO₂ values generally agree fairly well with observations except in fall when field data are significantly higher than modelled values. Over the winter season, modelled surface pCO₂ are close to saturation (Fig. 4c). A marked decrease of pCO₂ is simulated in early March and coincides with the onset of the diatom bloom (Fig. 4c; Fig. 3a) and pCO₂ reaches its minimum (145 ppm) during the *Phaeocystis* bloom (Fig. 4c; Fig. 3b). Modelled pCO₂ increases as *Phaeocystis* declines and values above saturation with respect to atmospheric CO₂ are reached in July up to the end of October (Fig. 4c). The model early decrease of surface water pCO₂ in September compared to observations might be due to some underestimation of modelled bacterial biomass (and related activity) during fall (Fig. 3d).

3.2 Carbon budget

An annual budget of C flows was constructed for BCZ based on time integration of MIRO daily simulations of biological activities (photosynthesis and planktonic and benthic respiration), Atlantic inputs, Scheldt loads and air-sea CO₂ fluxes. Results of these calculations (Fig. 5)

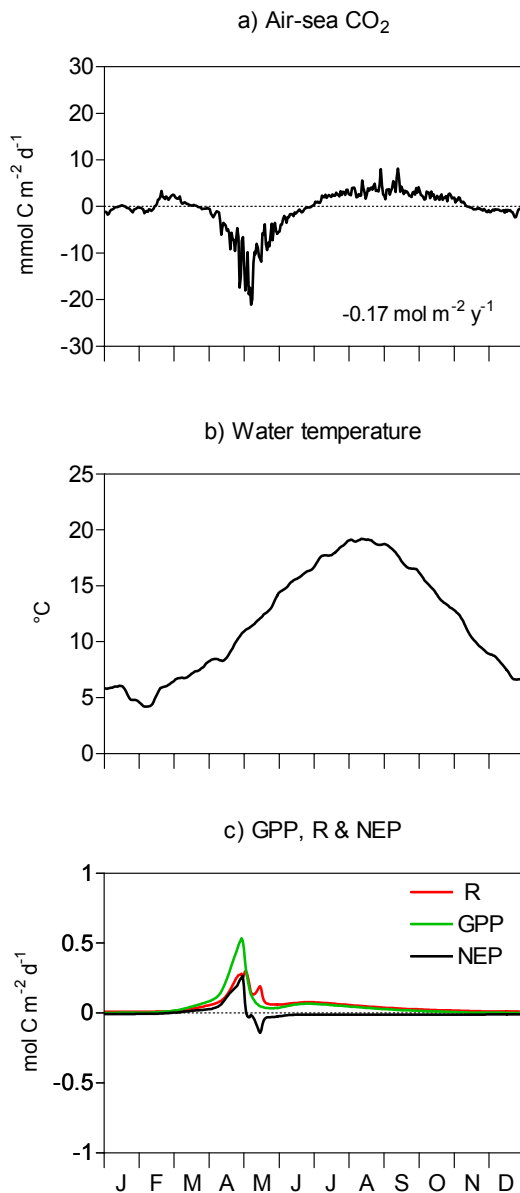


Fig. 6. Seasonal evolution of (a) modelled air-sea CO₂ flux, (b) mean water temperature for the 1996–1999 period and (c) gross primary production (GPP), total respiration (R) and net ecosystem production (NEP) computed for BCZ from MIRO-CO₂ daily simulations of biological activities.

highlight the importance of Atlantic inputs of inorganic (226.26 mol C m⁻² y⁻¹) and organic (10.63 mol C m⁻² y⁻¹) carbon representing, respectively, 95 and 99% of total inputs to BCZ. River Scheldt inputs contributes to 4.5 and 1% of total DIC and TOC inputs, respectively. The uptake of atmospheric CO₂ is low (-0.17 mol C m⁻² y⁻¹) i.e. less than 0.1% of the total input of DIC. Autotrophic processes fix some 8% of the annual input of DIC (18.79 mol C m⁻² y⁻¹) from which 77 and 20% is remineralized in the water column

and sediment, respectively (Fig. 5). At the annual scale BCZ exports to the North some 0.38 mol C m⁻² y⁻¹ as TOC while little carbon is buried in the sediment (0.01 mol C m⁻² y⁻¹).

3.3 Physical and biological controls of surface water pCO₂ and air-sea CO₂ fluxes in central BCZ at the seasonal and annual scales

Physical and biological mechanisms regulating pCO₂ (Fig. 4c) and air-sea exchanges of CO₂ (Fig. 6a) in central BCZ were first investigated based on the comparative analysis of MIRO-CO₂ daily forcing of temperature (Fig. 6b) and predictions of biological features (gross primary production GPP, community respiration R (including autotrophic and heterotrophic planktonic and benthic respiration) and net ecosystem production NEP (the difference between GPP and R), Fig. 6c). In winter (November to late February), NEP and R are close to zero (Fig. 6c) and pCO₂ fluctuations (Fig. 4c) are modulated by river inputs of carbon and seawater temperature (Fig. 6b). The system is near equilibrium and air-sea CO₂ fluxes are close to zero (Fig. 6a). From mid-March to end April, NEP is high enough to reverse the positive effect of temperature increase on pCO₂ that reaches extremely low values with respect to saturation (Fig. 4c; Fig. 6b, c). In accordance, our model calculates for this period an important sink of atmospheric CO₂ in central BCZ (up to -20 mmol C m⁻² d⁻¹; Fig. 6a). In May, NEP is strongly negative (i.e. the system is heterotrophic) and surface water pCO₂ increases due to both respiration and temperature increase (Fig. 4c; Fig. 6b, c). As a consequence the system evolves progressively from a sink of atmospheric CO₂ during spring to a source during the period end of June to November (Fig. 6a). After November, the system is again close equilibrium (Fig. 6a). Overall MIRO-CO₂ estimates a weak annual sink of atmospheric CO₂ of -0.17 mol C m⁻² y⁻¹.

As a first attempt to appraise the relative importance of physical and biological controls of surface water pCO₂, we used the approach of Takahashi et al. (2002) that separates the seasonal effect of ‘net biology’ from that of temperature. As defined by these authors the ‘net biology’ effect includes the effect of biological processes, TA variation due to nitrate utilization, air-sea exchange of CO₂ and an addition of DIC and TA by external forcing (river inputs in the present study). Removal of the temperature effect on pCO₂ simulations is obtained after normalization of modelled daily values of pCO₂ to the annual mean temperature (11.9°C) using the equation:

$$p\text{CO}_2 \text{ at } T_{\text{mean}} = p\text{CO}_2_{\text{mod}} \cdot \exp[0.0423 \cdot (T_{\text{mean}} - T_{\text{mod}})], \quad (1)$$

where T_{mean} and T_{mod} are, respectively, the climatological annual mean and daily temperature (in °C) used in model runs.

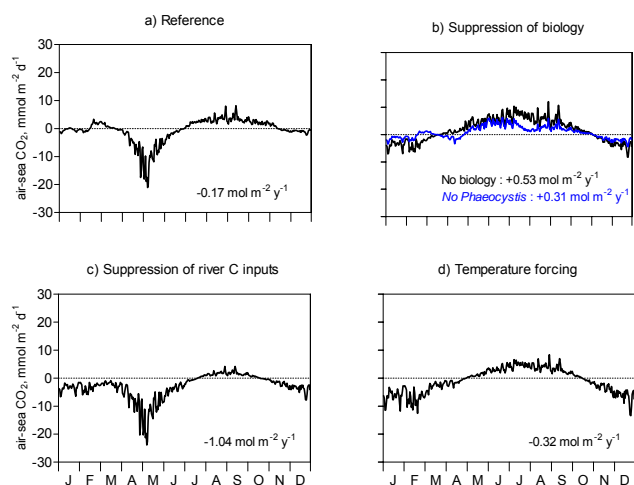


Fig. 7. Seasonal evolution of MIRO-CO₂ pCO₂ computed for (a) the reference run and by closing (b) biological processes or only *Phaeocystis* growth, (c) river inputs of inorganic and organic carbon or (d) both biological processes and carbon inputs. The annual integrated CO₂ air-sea flux calculated for each scenario is indicated on the corresponding plot.

The seasonal effect of temperature on pCO₂ is further estimated by attributing to the mean annual pCO₂ deduced from model runs (i.e. 360 ppm) a correction factor based on the difference between T_{mod} and T_{mean} as above. According to these calculations, the effect of biology on pCO₂, represented by the seasonal amplitude of pCO₂ values corrected to the mean annual temperature, is estimated at 350 ppm (150 ppm in May to 500 ppm in February). The effect of temperature change is less, 230 ppm (260 ppm in January-February to 490 ppm in July-August). The relative importance of the temperature and ‘net biology’ effect (T/B) is given by the ratio between the above seasonal amplitudes and is evaluated at 0.66. Thus, based on MIRO-CO₂ results we conclude that temperature contributed less to the seasonal pCO₂ variability of central BCZ in 1996–1999 than biological processes. However in areas influenced by river inputs of carbon and nutrients such as BCZ, the approach of Takahashi et al. (2002) includes their impact in the so-called ‘net biology’ effect.

As an alternate approach to resolve these contributions, we compared MIRO-CO₂ reference 1996–1999 simulations of the seasonal evolution of surface water pCO₂ in BCZ and the related annual air-sea CO₂ fluxes (Fig. 7a) with those obtained by closing separately biological processes, *Phaeocystis* only (Fig. 7b) and the river inputs of organic and inorganic carbon (Fig. 7c). For the latter scenario the river nutrient inputs were maintained. A supplementary MIRO-CO₂ scenario with closing both biological processes and river inputs of carbon was conducted to extract the solely thermodynamic effect of temperature change on pCO₂ (Fig. 7d).

Suppressing biological processes predicts in BCZ a significant annual source of atmospheric CO₂ (+0.53 mol C m⁻² y⁻¹

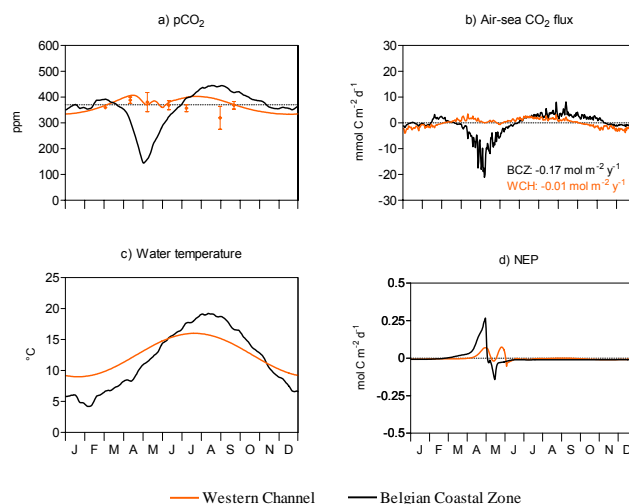


Fig. 8. Seasonal evolution of MIRO-CO₂ simulations of daily (a) pCO₂, (b) air-sea CO₂ flux, (c) water temperature and (d) net ecosystem production computed for WCH and BCZ boxes. Model results of pCO₂ in WCH (solid line) are compared with available observations in that area (♦). The dotted line, in the pCO₂ plots, corresponds to atmospheric pCO₂. The calculated annual CO₂ air-sea flux is added to each plot of air-sea CO₂ flux.

y⁻¹, Fig. 7b). This suggests that biology is responsible for the annual sink predicted in BCZ (Fig. 7a) by taking up to 0.7 mol C m⁻² y⁻¹ of atmospheric CO₂. In the absence of biology, seasonal evolution of water pCO₂ is mainly determined by temperature and water CO₂ super-saturation with respect to the atmosphere is simulated in summer (Fig. 7b) when water temperature is elevated (Fig. 6b). Additional comparison with scenarios closing separately *Phaeocystis* colonies estimates at more than 50% the contribution of their bloom to this uptake (−0.47 mol C m⁻² y⁻¹, Fig. 7b). Comparison with the reference run (Fig. 6a) indicates that the simulated water CO₂ under-saturation in spring is mainly associated with *Phaeocystis* colony growth. Spring diatoms also contribute to spring water CO₂ undersaturation (Fig. 7b) but to a lesser extent. Suppression of river inputs of organic and inorganic carbon has no detectable influence on the seasonal evolution of pCO₂ but increases significantly the annual CO₂ sink obtained with the reference run (Fig. 7a, c). River inputs of carbon thus represent a significant source of atmospheric CO₂ (+0.87 mol C m⁻² y⁻¹) that is partly counteracted by biology on an annual scale (−0.7 mol C m⁻² y⁻¹). Finally our scenarios predict an annual sink of atmospheric CO₂ of −0.32 mol C m⁻² y⁻¹ associated to the seasonal signal of temperature only (Fig. 7d). All together these scenarios shows the predominance of different controls of pCO₂ and air-sea CO₂ exchanges in central BCZ along the season. Clearly river inputs of carbon are responsible for the simulated emission of CO₂ to the atmosphere in late winter, counteracting the effect of decreasing temperature (Fig. 7c,

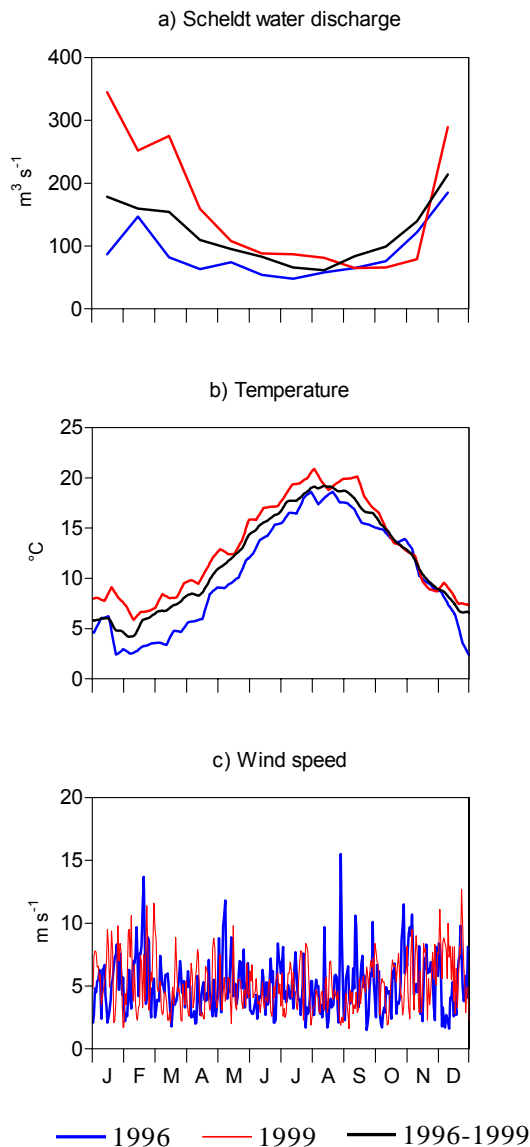


Fig. 9. Seasonal cycle of (a) Scheldt fresh water discharge, (b) water temperature and (c) wind speed for 1996 and 1999 compared to the climatological reference (for (a) Scheldt discharge and (b) water temperature).

d). NEP mostly that associated to *Phaeocystis* colonies explains the predicted CO₂ sink in spring which, under these conditions of temperature should have been a CO₂ source towards the atmosphere (Fig. 7a, b). During summer, temperature first and then C remineralization are the most important controls (Fig. 7b, d).

3.4 Role of land-based nutrients

In order to better appraise the role of land-based nutrients and carbon in modulating the seasonal cycle of surface water pCO₂ and air-sea CO₂ fluxes, we compared model

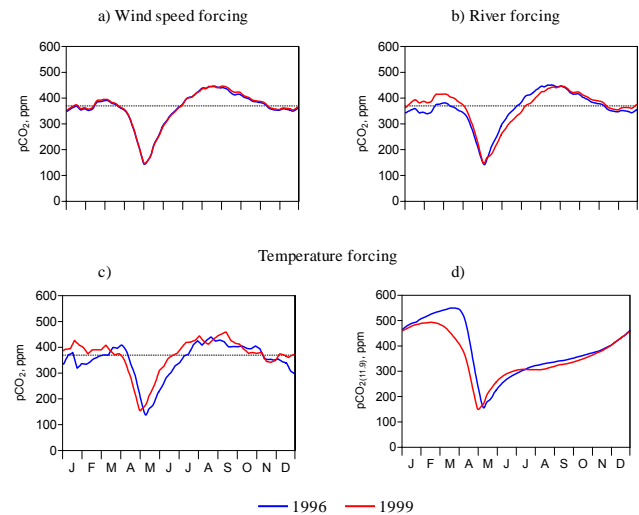


Fig. 10. Seasonal evolution of MIRO-CO₂ pCO₂ obtained with changing (a) wind speed, (b) river carbon and nutrient loads (c) water temperature of 1996 and 1999 and (d) same as (c) but normalized to BCZ average temperature of 11.9°C. The dotted line corresponds to atmospheric equilibrium.

results in central BCZ with those obtained for the WCH boundary conditions (Fig. 8). For this purpose simulations of pCO₂ (Fig. 8a) and air-sea CO₂ exchanges (Fig. 8b) in both areas were compared with the temperature forcing (Fig. 8c) and the simulated NEP (Fig. 8d). In the WCH, a fairly good agreement is observed between daily simulations of pCO₂ and available field data (Fig. 8a). As a general trend surface water pCO₂ in WCH is driven by temperature variation, being under-saturated with respect to the atmosphere between October and mid-March and over-saturated during spring-summer (Fig. 8a). Over the latter period, two small decreases in pCO₂ are simulated, coinciding with events of elevated NEP (Fig. 8d) that are counteracting the effect of temperature increase (Fig. 8a, c, d). However and contrary to BCZ, the simulated pCO₂ never reaches under-saturated values in spring due to the low productivity of WCH compared to BCZ (Fig. 8a). At the annual scale indeed BCZ is net autotrophic (integrated NEP=+0.38 mol C m⁻² y⁻¹) while WCH is close to metabolic balance (integrated NEP ~0 mol C m⁻² y⁻¹). Accordingly, WCH is almost in equilibrium with respect to atmospheric CO₂ (-0.01 mol C m⁻² y⁻¹; Fig. 8b) when BCZ acts as a sink for atmospheric CO₂ (-0.17 mol C m⁻² y⁻¹).

Applying the approach of Takahashi et al. (2002) to WCH simulations allows us to conclude that temperature variation over the year contributes more to pCO₂ seasonal variation than biology (T/B=1.21). Comparing this result with T/B obtained in BCZ (0.66) points to the major contribution of nutrient river inputs (i.e. coastal eutrophication) in counteracting the temperature control on surface water pCO₂.

Table 1. Comparison between annual integrations of air-sea CO₂ fluxes, gross primary production (GPP), respiration (R) and net ecosystem production (NEP) computed for the reference run (1996–1999) and those obtained with separate modification to the reference of 1996 and 1999 river nutrient and carbon loads or temperature or wind speed forcing. The relative importance of temperature and biology effect on pCO₂ is expressed by the ratio T/B.

	Reference	Wind speed		River discharge		Temperature	
	1996–1999	1996	1999	1996	1999	1996	1999
Air-sea CO ₂ flux, mol C m ⁻² y ⁻¹	−0.17	−0.20	−0.14	−0.24	−0.05	−0.39	+0.04
GPP, mol C m ⁻² y ⁻¹	18.8	18.8	18.8	17.2	21.9	17.1	19.7
R, mol C m ⁻² y ⁻¹	18.4	18.4	18.4	16.9	21.4	16.7	19.3
NEP, mol C m ⁻² y ⁻¹	+0.38	+0.38	+0.38	+0.32	+0.56	+0.44	+0.42
T/B	0.66	0.66	0.65	0.68	0.6	0.68	0.69

3.5 Sensitivity to external present-day forcings

In this section we explore to what extent changing meteorological conditions (rainfall (i.e. river discharge), temperature, wind stress) could alter the seasonal and annual dynamics of pCO₂ in coastal waters. For this application, we choose to compare MIRO-CO₂ reference simulations relative to the 1996–1999 climatological year with results obtained when running the model with changing one by one either the river inputs of carbon or the water temperature or the wind speed forcing corresponding to the most contrasted “meteorological” years for the period (the dry 1996 and wet 1999 year). For each simulation, the other forcing were maintained equal to the reference 1996–1999 mean value. Over 1996–1999, nutrient loads were very variable, modulated by freshwater discharge that was higher in 1999 compared to 1996 (Fig. 9a). Nutrient concentrations in the Seine and Scheldt rivers were indeed unchanged over this period. Similarly, concentrations of organic and inorganic carbon were assumed constant. Significantly higher temperatures were observed in 1999 compared to 1996, especially between January and August (Fig. 9b). Daily wind speeds were quite variable with however a similar annual average of 5.05 and 5.16 m s⁻¹ in 1996 and 1999, respectively (Fig. 9c).

The relative impact of each forcing was explored based on a comparison of modelled pCO₂ along the season (Fig. 10) and MIRO-CO₂ annual budget of biological activity (GPP, R and NEP) and air-sea CO₂ flux (Table 1). Generally, the seasonal trends and magnitude of pCO₂ variations were not significantly modified. However, significant changes in the intensity and direction of the annual air-sea CO₂ flux were simulated (Table 1).

3.5.1 Wind speed forcing

We found a negligible effect of wind speed on the seasonal cycle of pCO₂ (Fig. 10a), since this forcing does not control NEP and temperature in our model (Table 1). Still, these model scenarios reveal that the daily variations of wind speed impacted significantly on the annual budget of air-sea

CO₂ (18%; Table 1). The largest sink is predicted in 1996 (−0.2 mol C m⁻² y⁻¹, Table 1) and corresponds to lower gas transfer velocity, (8.38 and 8.58 cm h⁻¹ (normalized to a Schmidt number of 600) in 1996 than in 1999, respectively).

3.5.2 River forcing

Comparison of seasonal simulations of water pCO₂ obtained with 1996 and 1999 river loads, shows for 1996 lower values between January and March, similar in May and higher from May to August (Fig. 10b). The lower late winter pCO₂ simulated in 1996 are mostly due to the lower DIC river inputs as biological activity in winter is low. The initial winter pCO₂ value in 1996 also probably explains why minimal pCO₂ values simulated in spring are very similar for both years (Fig. 10b), although the maximum NEP value obtained during the *Phaeocystis* bloom is higher in 1999 than 1996 (0.28 mol C m⁻² d⁻¹ in 1999 compared to 0.21 mol C m⁻² d⁻¹ in 1996, not shown).

On an annual base we calculated a lower sink for atmospheric CO₂ in 1999 compared to 1996 (Table 1) which contrasts with the elevated NEP simulated in 1999 (Table 1) in response to the higher riverine nutrient inputs. This has to be related to the higher DIC river inputs in 1999 that induce higher initial pCO₂ values in winter (Fig. 10b). Altogether this scenario points the dual role of river inputs on the seasonal dynamics of pCO₂ in eutrophied coastal waters by modulating their carbon and nutrient conditions.

3.5.3 Temperature forcing

Clearly, the difference in time and magnitude of surface water pCO₂ simulated in 1996 and 1999 (Fig. 10c) corresponds with temperature records deviation over the period January-to-July (Fig. 9b). Over this period temperature is significantly higher in 1999 than in 1996 (~3°C, Fig. 9b). In order to eliminate the temperature effect, modelled pCO₂ were normalized to the mean BCZ temperature (11.9°C, Fig. 10d). From January to February, the lower pCO₂ simulated in 1996 are clearly due to lower temperature compared to 1999

(Fig. 10d). The 9 days delay obtained for the minimal simulated pCO₂ values in spring (Fig. 10d) is related to the late onset of *Phaeocystis* bloom in 1996 as a consequence of the temperature dependence of GPP. On an annual base, NEP is lower in 1999 than in 1996 (Table 1), in spite of a higher GPP in 1999 than in 1996 (Table 1), due to the stronger temperature dependence of heterotrophic processes.

The shift from an annual sink in 1996 to a source in 1999 of atmospheric CO₂ (Table 1) is related to a combination of temperature effect on the carbon chemistry and biology (increased respiration at higher temperature). Their relative importance can be assessed through the calculation of the T/B i.e. the ratio between $\Delta p\text{CO}_2(\text{temp})$ and $\Delta p\text{CO}_2(\text{bio})$ (Table 1). This suggests a higher temperature effect on biology than carbon chemistry. Indeed the T/B increase from 0.68 in 1996 to 0.69 in 1999 (Table 1) is due to a higher difference between $\Delta p\text{CO}_2(\text{bio})$ (362 ppm in 1996 compared to 353 ppm in 1999) than $\Delta p\text{CO}_2(\text{temp})$ (247 ppm in 1996 and 244 ppm in 1999).

4 Conclusions

The MIRO-CO₂ simulations, by showing stronger seasonal signals of pCO₂ and related air-sea CO₂ fluxes in the carbon and nutrient-enriched BCZ compared to more oceanic waters (WCH), is giving additional support to observation-based conclusions on the key role of coastal areas in the global carbon cycle (e.g. Frankignoulle and Borges, 2001a). We also demonstrated the advantage of model simulations and sensitivity analysis for the identification of the major physical and biological mechanisms controlling the seasonal dynamics of surface water pCO₂ and their external forcing. In particular, we highlighted the significance of the *Phaeocystis* bloom in the spring-time drawn-down of atmospheric CO₂. The model also allows us to explore how the intensity and direction of the annual air-sea CO₂ flux was changed in relation to realistic variations of environmental forcing such as water temperature, fresh water discharge or wind speed.

Model results revealed that the seasonal variation of pCO₂ in the BCZ is strongly driven by nutrient-enriched biological activity in spring that counteracts the effect of temperature increase. On an annual scale for the 1996–1999 period, the solely river inputs of organic and inorganic carbon are driving a source of CO₂ of +0.87 mol C m⁻² y⁻¹ that is balanced by an atmospheric CO₂ uptake of -0.7 and -0.32 mol C m⁻² y⁻¹ due to nutrient stimulated NEP and temperature change, respectively. Globally an annual weak sink is predicted for BCZ. However, based on a sensitivity analysis, we also showed that the present-day interannual variations of fresh water discharge (and related land-based nutrient and carbon inputs) and water temperature might have a significant impact on the air-sea CO₂ fluxes in the BCZ.

These simulations clearly illustrate the potentially significant but complex variations of CO₂ fluxes in near-shore coastal ecosystems in response to small environmental changes within the range of present-day variability. These variations in CO₂ fluxes are a small glimpse of those that can be expected from environmental changes predicted in the near future in context of global change and/or of management strategies.

Acknowledgements. This work was carried out in the framework of the Belgium Federal Science Policy projects AMORE (EV/11/19) and CANOPY (EV/03/20), the EU-FP5 project EUROTROPH (EVK3-CT-2000-00040) and the project 2.4545.02 of the Fonds National de la Recherche Scientifique (FNRS). DIC and TA data in the Seine estuary were kindly provided by G. Abril (Département de Géologie et Océanographie, Université de Bordeaux 1). N. Gypens has financial support from the 'Fond pour la Formation à la Recherche dans l'Industrie et dans l'Agriculture' (FRIA, FNRS, Belgium). We also acknowledge the reviewers for their constructive feedback.

Edited by: J. Middelburg

References

- Billen, G. and Servais, P.: Modélisation des processus de dégradation bactérienne de la matière organique en milieu aquatique, In: *Micro-organismes dans les écosystèmes océaniques* (Bianchi, M., Marty, D., Bertrand, J.-C., Caumette, P., and Gauthier, M.), edited by: Masson, 219–245, 1989.
- Borges, A. V. and Frankignoulle, M.: Daily and seasonal variations of the partial pressure of CO₂ in the surface seawater along Belgian and southern Dutch coastal areas, *J. Mar. Syst.*, 19, 251–266, 1999.
- Borges, A. V. and Frankignoulle, M.: Distribution of surface carbon dioxide and air-sea exchange in the upwelling system off the Galician coast, *Global Biogeochem. Cycles*, 16 (2), art.-no. 1020, 1–14, 2002a.
- Borges, A. V. and Frankignoulle, M.: Distribution and air-water exchange of carbon dioxide in the Scheldt plume off the Belgian coast, *Biogeochemistry*, 59, 41–67, 2002b.
- Borges, A. V. and Frankignoulle, M.: Distribution of surface carbon dioxide and air-sea exchange in the English Channel and adjacent areas, *J. Geophys. Res.*, 108 (C8), 3140, doi:10.1029/2000JC000571, 2003.
- Borges, A. V., Djenidi, S., Lacroix, G., Théate, J.-M., Delille, B., and Frankignoulle, M.: CO₂ atmospheric flux from mangrove surrounding waters, *Geophys. Res. Lett.*, 30 (11), 1558, doi:10.1029/2003GL017143, 2003.
- Bouillon, S., Frankignoulle, M., Dehairs, F., Velimirov, B., Eiler, A., Abril, G., Etcheber, H., and Borges, A. V.: Inorganic and organic carbon biogeochemistry in the Gautami Godavari estuary (Andhra Pradesh, India) during pre-monsoon: the local impact of extensive mangrove forests, *Global Biogeochem. Cycles*, 17 (4), 1114, doi:10.1029/2002GB002026, 2003.
- Brasse, S., Nellen, M., Seifert, R., and Michaelis, W.: The carbon dioxide system in the Elbe estuary, *Biogeochemistry*, 59 (1–2), 25–40, 2002.

- Cai, W. J., Wiebe, W. J., Wang, Y. C., and Sheldon, J. E.: Intertidal marsh as a source of dissolved inorganic carbon and a sink of nitrate in the Satilla River-estuarine complex in the southeastern US, *Limnol. Oceanogr.*, 45 (8), 1743–1752, 2000.
- Cai, W.-J., Wang, Z. A., and Wang, Y.: The role of marsh-dominated heterotrophic continental margins in transport of CO₂ between the atmosphere, the land-sea interface and the ocean, *Geophys. Res. Lett.*, 30, 3–1/3–4, 2003.
- DeGrandpre, M. D., Olbu, G. J., Beatty, C. M., and Hammar, T. R.: Air-sea CO₂ fluxes on the US Middle Atlantic Bight, *Deep-Sea Research Part II, Topical Studies in Oceanography*, 49 (20), 4355–4367, 2002.
- Frankignoulle, M. and Borges, A. V.: European continental shelf as a significant sink for atmospheric carbon dioxide, *Global Biogeochem. Cycles*, 15 (3), 569–576, 2001a.
- Frankignoulle, M. and Borges, A. V.: Direct and indirect pCO₂ measurements in a wide range of pCO₂ and salinity values (the Scheldt estuary), *Aquatic Geochemistry*, 7, 267–273, doi:10.1023/A:1015251010481, 2001b.
- Frankignoulle, M., Bourge, I. and Wollast, R.: Atmospheric CO₂ fluxes in a highly polluted estuary (The Scheldt), *Limnology and Oceanography*, 41 (2), 365–369, 1996.
- Frankignoulle, M., Abril, G., Borges, A. V., Bourge, I., Canon, C., Delille, B., Libert, E., and Théate, J.-M.: Carbon dioxide emission from European estuaries, *Science*, 282, 434–436, 1998.
- Gattuso, J.-P., Frankignoulle, M., and Wollast, R.: Carbon and carbonate metabolism in coastal aquatic ecosystems, *Ann. Rev. Ecol. Syst.*, 29, 405–433, 1998.
- Hannon, E., Boyd, P. W., Silviso, M., and Lancelot, C.: Modelling the bloom evolution and carbon flows during SOIREE: Implications for future in situ iron-experiments in the Southern Ocean, *Deep-Sea Research II*, 48, 2745–2773, 2001.
- Hoppema, J. M. J.: The seasonal behaviour of carbon dioxide and oxygen in the coastal North Sea along the Netherlands, *Netherlands Journal of Sea Research*, 28 (3), 167–179, 1991.
- Ianson, D. and Allen, E.: A two-dimensional nitrogen and carbon flux model in a coastal upwelling region, *Global Biogeochem. Cycles*, 6 (1), 1011, doi:10.1029/2001GB0001451, 2002.
- Kaul, L. and Froelich, P.: Modelling estuarine nutrient biogeochemistry in a simple system, *Geochim. Cosmochim. Acta*, 48, 1417–1433, 1984.
- Lancelot, C.: The mucilage phenomenon in the continental coastal waters of the North Sea, *The Science of the Total Envir.*, 165, 83–102, 1995.
- Lancelot, C., Billen, G., Sourmia, A., Weisse, T., Colijn, F., Veldhuis, M., Davies, A., and Wassmann, P.: Phaeocystis blooms and nutrient enrichment in the continental coastal zone of the North Sea, *Ambio*, 16 (1), 38–46, 1987.
- Lancelot, C., Spitz, Y., Gypens, N., Ruddick, K., Becquevort, S., Rousseau, V., Lacroix, G., and Billen, G.: Modelling diatom-Phaeocystis blooms and nutrient cycles in the Southern Bight of the North Sea with focus on the Belgian coastal zone: the MIRO model, *Mar. Ecol. Prog. Syst.*, accepted, M5518, 2004.
- Mackenzie, F. T., Lerman, A., and Andersson, A. J.: Past and present of sediment and carbon biogeochemical cycling models, *Biogeosciences*, 1, 11–32, 2004, **SRef-ID: 1726-4189/bg/2004-1-11.**
- Millero, F. J., Zhang, J.-Z., Fiol, S., Sotolongo, S., Roy, R. N., Lee, K., and Mane, S.: The use of buffers to measure pH in seawater, *Marine Chemistry*, 44, 143–152, 1993.
- Nightingale, P. D., Malin, G., Law, C. S., Watson, A. J., Liss, P. S., Liddicoat, M. I., Boutin, J., and Upstill-Goddard, R. C.: In-situ evaluation of air-sea gas exchange parametrizations using novel conservative and volatile tracers, *Global Biogeochem. Cycles*, 14, 373–387, 2000.
- Radach, G., Pätsch, J., Gekeler, J., and Herbig, K.: Annual cycles of nutrients and chlorophyll in the North Sea, *Ozeanographie Berichte 20*, Zentrum für Meeres- und Klimaforschung, 1995.
- Raymond, P. A., Bauer, J. E., and Cole, J. J.: Atmospheric CO₂ evasion, dissolved inorganic carbon production, and net heterotrophy in the York River estuary, *Limnol. Oceanogr.*, 45 (8), 1707–1717, 2000.
- Rousseau, V.: Dynamics of Phaeocystis and diatom blooms in the eutrophicated coastal waters of the Southern Bight of the North Sea, PhD Thesis, Université Libre de Bruxelles, Belgium, 205, 2000.
- Servais, P., Mercier, P., and Anzil, A.: Activité hétérotrophe et biodégradabilité de la matière organique dans la zone de turbidité maximale de l'estuaire de Seine, *Programme Seine-Aval*, 2003.
- Takahashi, T., Sutherland, S. C., Sweeney, C., Poisson, A., Metzl, N., Tilbrook B., Bates, N., Wanninkhof, R., Feely, R. A., Sabine, C., Olafsson, J., and Nojiri, Y.: Global sea-air CO₂ flux based on climatology of surface ocean pCO₂, and seasonal biological and temperature effects, *Deep-sea Research II*, 49, 1601–1622, 2002.
- Takahashi, T., Sutherland, S. C., Feely, R. A., and Cosca, C. E.: Decadal variation of the surface water pCO₂ in the western and central equatorial Pacific, *Science*, 302 (5646), 852–856, 2003.
- Thomas, H., Bozec, Y., Elkalay, K., and de Baar, H. J. W.: Enhanced open ocean storage of CO₂ from shelf sea pumping, *Science*, 304, 1005–1008, 2004a.
- Thomas, H., Bozec, Y., de Baar, H., Elkalay, K., Frankignoulle, M., Schiettecatte, L.-S., and Borges, A. V.: The Carbon budget of the North Sea, *Biogeosciences Discussions*, 1, 367–392, 2004b, **SRef-ID: 1810-6285/bgd/2004-1-367.**
- Tsunogai, S., Watanabe, S., and Sato, T.: Is there a “continental shelf pump” for the absorption of atmospheric CO₂?, *Tellus Series B-Chemical and Physical Meteorology*, 51 (3), 701–712, 1999.
- Walsh, J. J. and Dieterle, D. A.: CO₂ cycling in the coastal ocean, I – A numerical analysis of the Southeastern Bering Sea with applications to the Chukchi Sea and the northern Gulf of Mexico, *Prog. Oceanog.*, 34, 335–392, 1994.
- Walsh, J. J., Dieterle, D. A., Muller-Karger, F. E., Aagaard, K., Roach, A. T., Whitledge, T. E., and Stockwell, D.: CO₂ cycling in the coastal ocean, II. Seasonal organic loading of the Arctic Ocean from source waters in the Bering Sea, *Cont. Shelf Res.*, 17 (1), 1–36, 1996.
- Wang, Z. A. and Cai, W.-J.: Carbon dioxide degassing and inorganic carbon export from a marsh-dominated estuary (the Duplin River): A marsh CO₂ pump, *Limnol. Oceanogr.*, 49 (2), 341–354, 2004.
- Weiss, R. F.: Carbon dioxide in the water and seawater: the solubility of a non-ideal gas, *Marine Chemistry*, 2, 203–205, 1974.